10.1098/rsta.2000.0725

THE ROYAL SOCIETY

Hadron interactions and hadron structure

By W. James Stirling

Departments of Mathematical Sciences and Physics, University of Durham, Durham DH1 3LE, UK

While deep-inelastic scattering experiments are the primary source of information on the parton structure of hadrons, hard-scattering processes in hadron–hadron collisions also provide useful information. We describe the theoretical framework that relates hard-scattering cross-sections to parton distribution functions, and review some of the recent phenomenology.

Keywords: hadron structure; parton distributions; phenomenology

1. Introduction

It was first pointed out by Drell & Yan (1970) that parton model ideas developed for deep-inelastic scattering could be extended to certain processes in hadron–hadron collisions. The paradigm process, proposed by Drell & Yan, was the production of a massive lepton pair by quark–antiquark annihilation: the Drell–Yan process (illustrated in figure 1). For the production of a lepton pair of invariant mass M, the hadronic cross-section $\mathrm{d}\sigma/\,\mathrm{d}M^2$ was to be obtained by weighting the subprocess cross-section $\mathrm{d}\hat{\sigma}/\,\mathrm{d}M^2$ for $\mathrm{q\bar{q}} \to \mu^+\mu^-$

$$\frac{\mathrm{d}\hat{\sigma}}{\mathrm{d}M^2} = \frac{4\pi\alpha^2}{3M^2} e_\mathrm{q}^2 \delta(\hat{s} - M^2), \tag{1.1}$$

with the parton distribution functions $f_\mathrm{q}(x)$ extracted from deep-inelastic scattering. Labelling the quark (antiquark) momentum fractions by x_1 (x_2), and noting that $\hat{s} = x_1 x_2 s$, the cross-section is

$$\begin{aligned}\frac{\mathrm{d}^2\sigma}{\mathrm{d}M^2} &= \frac{4\pi\alpha^2}{3M^4} \int_0^1 \mathrm{d}x_1 \mathrm{d}x_2\, \delta(x_1 x_2 - \tau) \sum_\mathrm{q} e_\mathrm{q}^2 f_\mathrm{q}(x_1) f_{\bar{\mathrm{q}}}(x_2) \\ &= \frac{4\pi\alpha^2}{3M^4} \mathcal{F}(\tau) \quad \text{(scaling variable } \tau = M^2/s\text{)}. \end{aligned} \tag{1.2}$$

In the original derivation of this result by Drell & Yan, there was no additional '1/3' quark colour averaging factor, and in order to quantify the cross-section it was assumed that $f_\mathrm{q} = f_{\bar{\mathrm{q}}} = f$, hence $\mathcal{F} \sim F_2 \otimes F_2$, where F_2 is the deep-inelastic structure function. The domain of validity of (1.2) is the asymptotic 'scaling' limit M^2, $s \to \infty$, $\tau = M^2/s$ fixed, in which limit the cross-section $M^4 \mathrm{d}\sigma/\,\mathrm{d}M^2$ depends only on the dimensionless ratio τ. Scaling was subsequently confirmed experimentally (figure 2 shows an example), thus validating the parton-model treatment of large-mass lepton pair production.

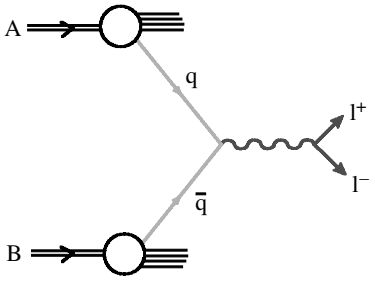

Figure 1. The Drell–Yan process.

The significance of the Drell–Yan process was that it showed for the first time that a rigorous, quantitative analysis of certain types of hadronic cross-section was possible. Studies were subsequently extended to other 'hard-scattering' processes, for example the production of hadrons with large transverse momentum and of heavy quarks, with equally successful results.

Drell & Yan (1970) realized the importance of hard-scattering processes for obtaining information on the parton structure of the colliding partons:

> The full range of processes of the type $A + B \to \mu^+\mu^- + \cdots$ with incident p, $\bar{p}$, π, K, γ, etc., affords the interesting possibility of comparing their parton and antiparton structures.

Indeed, nowadays data from hadron–hadron scattering processes are routinely used in 'global analyses' to determine the parton distribution functions of the proton (see, for example, the Martin–Roberts–Stirling–Thorne (MRST) work of Martin *et al*. (1998) or the Coordinated Theoretical–Experimental Project on QCD (CTEQ) work of Lai *et al*. 2000). As we shall see in the following sections, the Drell–Yan process provides essential information on the light quark sea in the proton and on the valence (quark and antiquark) distributions in the pion. The production of large transverse momentum jets and 'prompt' photons, on the other hand, is a vital source of information on the medium- and high-x *gluon* distribution in the proton.

In this brief review we will only have time to discuss the information on *quark* structure from hadron–hadron collisions. The extraction of the gluon distribution from large transverse momentum jet production at the Tevatron $p\bar{p}$ collider is described in Montgomery (this issue). Before discussing the phenomenology in more detail, we mention an important theoretical development of the 1970s that elevated the Drell–Yan cross-section from a byproduct of the original 'naive' parton model to a rigorous and central prediction of quantum chromodynamics (QCD).

2. QCD and factorization

In a quantum field theory such as QCD, in which quarks interact with massless (gluon) gauge bosons, figure 1 can be regarded as the leading-order (in the quark–gluon coupling) contribution to the inclusive process $q\bar{q} \to \mu^+\mu^- + X$. Problems arise, however, when perturbative corrections from real and virtual gluon emission are calculated. Large logarithms from gluons emitted collinear with the incoming quarks appear to spoil the convergence of the perturbative expansion. Writing the scaled

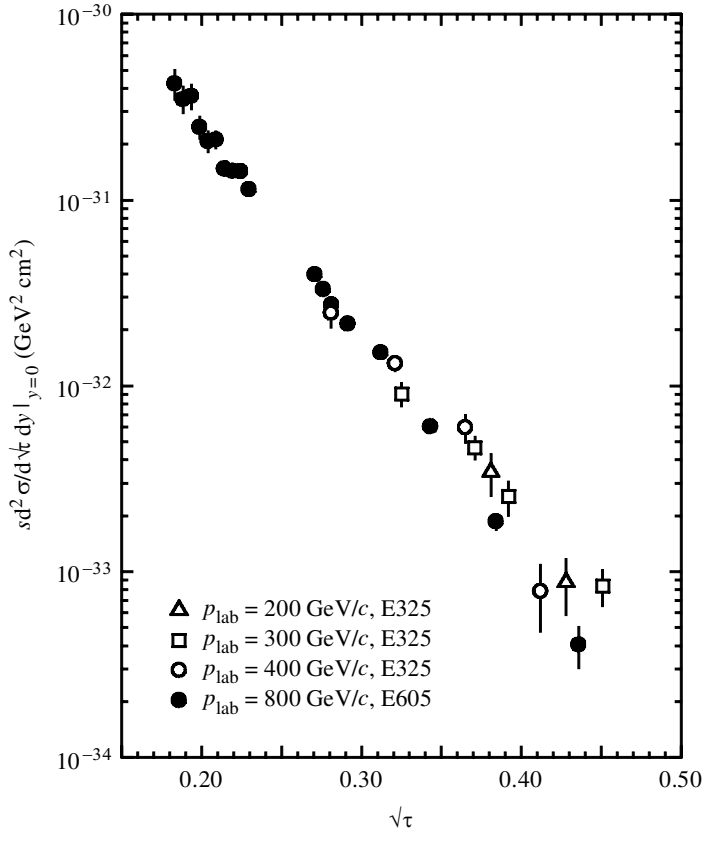

Figure 2. A comparison of Drell–Yan cross-sections at four different collision energies from two Fermilab experiments, E325 and E605 ($\mathrm{p} + \mathrm{Cu} \rightarrow \mu^+\mu^- + \mathrm{X}$). The cross-sections are seen to depend only on the variable τ, confirming the 'scaling' property.

parton-model Drell–Yan subprocess cross-section of equation (1.1) as $\hat{\mathcal{F}}_{\mathrm{q\bar{q}}} = \delta(1-\tau)$, then the $\mathcal{O}(\alpha_{\mathrm{s}})$ correction, calculated from the diagrams of figure 3, is†

$$\hat{\mathcal{F}}_{\mathrm{q\bar{q}}} = \delta(1-\tau) + \frac{\alpha_{\mathrm{s}}(\mu^2)}{2\pi}\left[2\ln\frac{Q^2}{\kappa^2}P^{(0)}_{\mathrm{qq}}(\tau) + C(\tau)\right] + \mathcal{O}(\alpha_{\mathrm{s}}^2), \tag{2.1}$$

where κ^2 is a dimensionful parameter introduced to regulate collinear divergences.

The key point, however, is that the coefficient of the logarithm in equation (2.1) is the same as that which arises in the analogous deep-inelastic scattering structure function calculation. It is therefore absorbed in the redefinition of the parton distributions, giving rise to logarithmic violations of scaling (see, for example, the discussion in Ellis *et al.* (1996)). In fact, *all* logarithms appearing in the Drell–Yan perturbative corrections can be factored into renormalized parton distributions in this way, and *factorization theorems*, which show that this is a general feature of hard-scattering processes, can be derived. Unlike the logarithmic corrections, the finite corrections such as $C(\tau)$ in equation (2.1) are process dependent, and modify the parton-model-like cross-section.

† Only the $\mathrm{q\bar{q}}$ corrections are exhibited here.

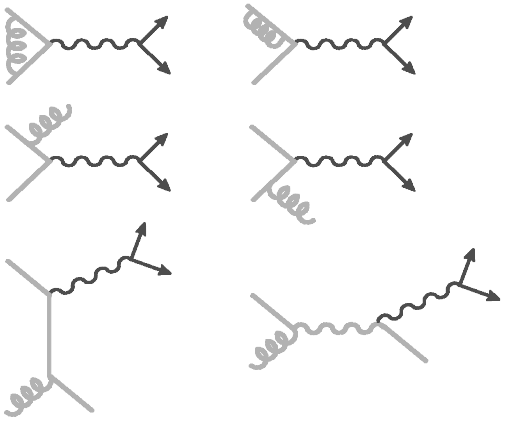

Figure 3. Next-to-leading-order diagrams for the Drell–Yan process.

The size of the perturbative corrections depends on the lepton-pair mass and on the overall centre-of-mass energy. At fixed-target energies and masses the correction is generally large and positive, of the order of 50% or more. In this regime of relatively large τ, the (negative) contribution from the quark–gluon scattering diagrams in figure 3 is quite small. However, at $\mathrm{p\bar{p}}$ collider energies, where τ is much smaller, the quark–gluon contribution is more important and the overall correction is smaller.

The general structure, valid for *any* hard-scattering process, is

$$\sigma_{\mathrm{AB}} = \sum_{\mathrm{a,b}} \int \mathrm{d}x_{\mathrm{a}} \mathrm{d}x_{\mathrm{b}}\, f_{\mathrm{a/A}}(x_{\mathrm{a}}, \mu_{\mathrm{F}}^2) f_{\mathrm{b/B}}(x_{\mathrm{b}}, \mu_{\mathrm{F}}^2) [\hat{\sigma}_0 + \alpha_{\mathrm{s}}(\mu_{\mathrm{R}}^2)\hat{\sigma}_1 + \cdots]_{\mathrm{ab}\to\mathrm{X}}. \quad (2.2)$$

Here μ_{F} is the *factorization scale* and μ_{R} is the *renormalization scale* for the QCD running coupling. Formally, the perturbation series is invariant under changes in these parameters, the μ_{F} and μ_{R} dependence of the coefficients, e.g. $\hat{\sigma}_1$, exactly compensating the explicit dependence of the parton distributions and the coupling constant. This compensation becomes more exact as more terms are included in the perturbation series. To avoid unnaturally large logarithms reappearing in the perturbation series it is sensible to choose μ_{F} and μ_{R} values of the order of the typical momentum scales of the hard-scattering process, for example $\mu_{\mathrm{F}} = \mu_{\mathrm{R}} = M$ for the Drell–Yan cross-section.

All the important hard-scattering hadronic processes have now been calculated to next-to-leading-order (NLO), i.e. up to and including the $\hat{\sigma}_1$ terms. One process, the Drell–Yan process, is even calculated to one order higher (see below). This allows a very high degree of precision in a wide variety of processes. In many cases, the residual renormalization and factorization scale dependence is weak, and the precision of the theoretical prediction is limited only by uncertainties in the knowledge of the parton distributions.

3. Hadron structure from the Drell–Yan process

(*a*) *Pion structure*

Hadron–hadron interactions are the *only* way to obtain direct information on the parton structure of mesons. There is a significant amount of data on hard-scattering

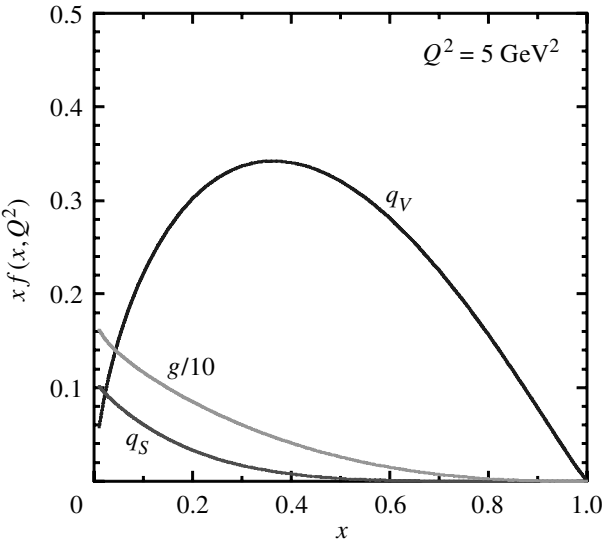

Figure 4. Parton distributions in the pion, from the analysis of Martin *et al.* (1992).

Table 1. *Moments of parton distributions in the pion, from the lattice calculation of Best et al. (1997) and the global fit of Martin et al. (1992)*

(PDF, parton distribution function.)

q_V moment	(quenched) lattice	MRSS PDF fit
$\langle x \rangle$	0.273 ± 0.012	0.228
$\langle x^2 \rangle$	0.107 ± 0.035	0.099
$\langle x^3 \rangle$	0.048 ± 0.020	0.055

processes like $\pi N \to (\mu^+\mu^-, \gamma, J/\psi, \dots) + X$. With the nucleon parton distributions determined from deep-inelastic scattering and other processes, the pion distributions can be extracted (Owens 1984; Aurenche *et al.* 1989; Martin *et al.* 1992; Glück *et al.* 1992). In this case Drell–Yan production is dominantly a valence–valence annihilation process. For the pion's *valence* quark distributions, therefore, the precision is essentially that of the input experimental data. It is much more difficult to extract precise information on the gluon and sea-quark distributions. Figure 4 shows the results of the global analysis of Martin *et al.* (1992). The sea-quark distribution is largely an educated (theoretical) guess.

In recent years there has been significant progress in calculating hadronic parton structure 'from first principles' using lattice QCD. Results exist for the first few moments of the polarized and unpolarized quark distributions in the pion in the so-called quenched approximation. Table 1 compares the lattice calculations of Best *et al.* (1997) with moments calculated from the valence quark distribution of figure 4. The agreement is reasonable, especially for the higher moments, which presumably are less affected by the quenched approximation (the 'missing' sea-quark distributions are expected to be significant only at small x).

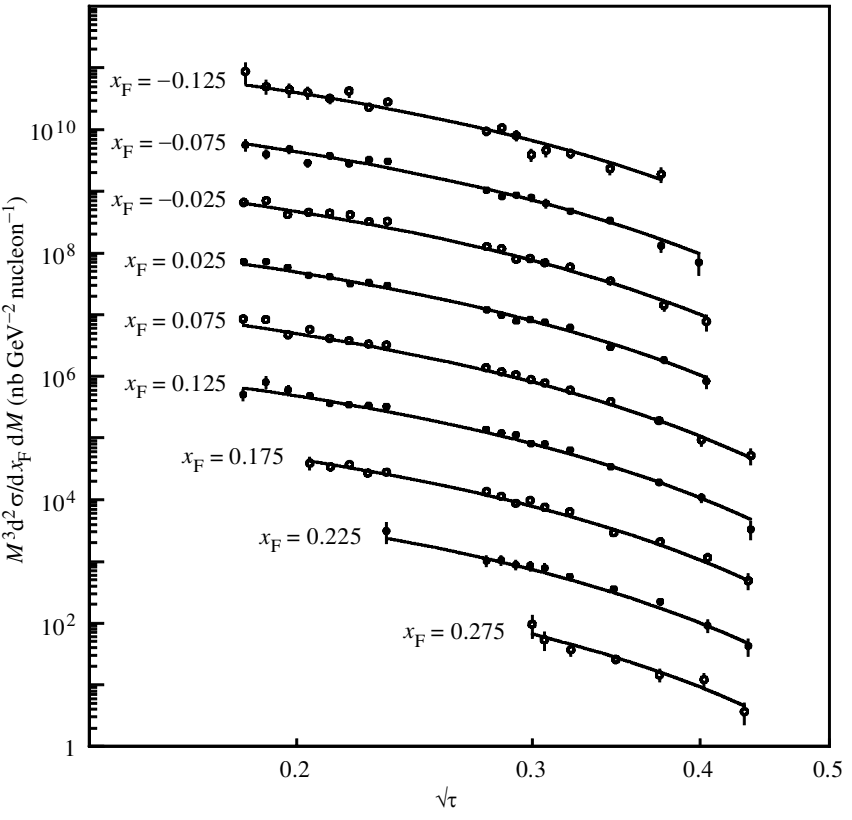

Figure 5. Cross-section $s\mathrm{d}^2\sigma/\,\mathrm{d}\sqrt{\tau}\,\mathrm{d}y$ for pCu $\to \mu^+\mu^-$X at $p_{\mathrm{lab}} = 800$ GeV/c ($\sqrt{s} = 38.8$ GeV) measured by the E605 collaboration (Moreno *et al.* 1991), with theoretical predictions from Martin *et al.* (1998) calculated at NLO.

(*b*) *The light quark sea in the proton*

In pp or pN collisions the cross-section is proportional to the sea-quark distribution, $\bar{\mathrm{q}}(x, \mu^2)$. This provides complementary information to deep-inelastic scattering, and in fact Drell–Yan data can be used to constrain the sea-quark distributions in global parton distribution fits. Most of the data are from fixed-target experiments using isoscalar targets, for which, to a good approximation, $\sigma_{\mathrm{pN}} \sim u_1(\bar{\mathrm{u}} + \bar{\mathrm{d}})_2$. It is therefore the *sum* of the light quark distributions that is probed.

Figure 5 shows an example of the use of high-precision Drell–Yan data in a global fit (Martin *et al.* 1998). Data from the E605 collaboration (Moreno *et al.* 1991) on the cross-section $s\mathrm{d}^2\sigma/\,\mathrm{d}\sqrt{\tau}\,\mathrm{d}y$ for pCu $\to \mu^+\mu^-$X at $p_{\mathrm{lab}} = 800$ GeV/c ($\sqrt{s} = 38.8$ GeV) are compared with theoretical predictions calculated at NLO. Here the u and d sea-quark distributions are adjusted to optimize the fit. The resulting agreement between theory and experiment is excellent, and suggests that the (unknown) higher-order corrections in this case are small.†

† An additional overall normalization factor is included in the fit, to allow for unknown higher-order corrections. The value of this factor was found by Martin *et al.* (1998) to be 1.07.

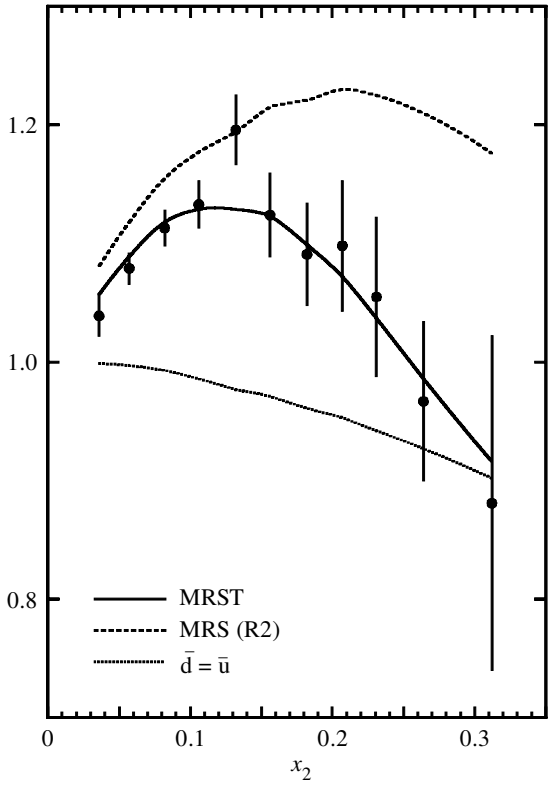

Figure 6. The MRST description (continuous curve) of the E866 data for the ratio of the proton and deuterium target Drell–Yan cross-sections versus x_2, the fractional momentum of the parton in the target ($\sigma^{pd}/2\sigma^{pp}$). The other curves are for comparison only.

(*c*) *The* $\bar{u}$, $\bar{d}$ *asymmetry in the quark sea*

It is difficult to determine $\bar{u}$ and $\bar{d}$ separately from deep-inelastic and isoscalar target Drell–Yan data. Indeed, before 1992, global parton analyses assumed that the non-strange sea was flavour symmetric, that is $\bar{u} = \bar{d}$. The first strong evidence that $\bar{u} \neq \bar{d}$ was the Gottfried sum measurement by NMC (Arneodo *et al.* 1994):

$$\int_0^1 \frac{dx}{x}(F_2^{\mu p} - F_2^{\mu n}) = \frac{1}{3} - \frac{2}{3}\int_0^1 dx\,(\bar{d} - \bar{u}) = 0.235 \pm 0.026, \tag{3.1}$$

which suggests

$$\int_0^1 dx\,(\bar{d} - \bar{u}) \approx 0.15.$$

Such a measurement, however, gives little information on the x dependence of the $\bar{d} - \bar{u}$ difference.

A powerful and independent method for obtaining further information on $\bar{d} - \bar{u}$ is to compare Drell–Yan lepton-pair production of pp and pd origin (Ellis & Stirling

1991). Defining the cross-section ratio

$$R_{\rm dp} \equiv \frac{\sigma_{\rm pd}}{2\sigma_{\rm pp}}, \tag{3.2}$$

it is straightforward to show that $R_{\rm dp} \approx 1$ if $\bar{\rm d} = \bar{\rm u}$. More generally,

$$\frac{\sigma_{\rm pd}}{2\sigma_{\rm pp}} \simeq 1 + \left\{ \frac{(4u_1 - d_1)(\bar{\rm d}_2 - \bar{\rm u}_2)}{4u_1\bar{\rm u}_2 + d_1\bar{\rm d}_2} \right\}, \tag{3.3}$$

where the 1, 2 subscripts indicate that the partons are to be evaluated at

$$x_1, x_2 = \tfrac{1}{2}(\pm x_{\rm F} + \sqrt{x_{\rm F}^2 + 4\tau}), \tag{3.4}$$

with $\tau = M^2/s$ and $x_{\rm F}$ the Feynman x of the produced lepton pair. Thus, by varying M and $x_{\rm F}$, the x dependence of $\bar{\rm d} - \bar{\rm u}$ can be measured.

The first experiment of this type was performed by the NA51 collaboration (Baldit *et al.* 1994) and yielded $\bar{\rm u}/\bar{\rm d} = 0.51 \pm 0.06$ at $x = 0.18$, $\mu^2 \sim 30\ {\rm GeV}^2$. More recently, the E866 collaboration (Hawker *et al.* 1998) have measured $R_{\rm dp}$ over a much wider range of M and $x_{\rm F}$, which enables a study of the x dependence of $\bar{\rm d} - \bar{\rm u}$ over the range $0.04 < x < 0.3$. The continuous curve in figure 6 shows the MRST fit (Martin *et al.* 1998) to these data. The dotted curve shows the $\bar{\rm d} = \bar{\rm u}$ prediction for the ratio. The implications for $\bar{\rm d}/\bar{\rm u}$ are shown in figure 7. Interestingly, the structure of $\bar{\rm d}/\bar{\rm u}$ shows that, at the maximum value of x that is measured, the ratio has decreased to give $\bar{\rm d} \simeq \bar{\rm u}$. Moreover, we see that the NA51 measurement occurs at a value of x for which $\bar{\rm d}/\bar{\rm u}$ is essentially at a maximum. Nevertheless, the new data indicate a somewhat smaller value of $\bar{\rm d}/\bar{\rm u}$ at this point, $x = 0.18$.

Despite much theoretical work, largely inspired by the recent Drell–Yan data, the origin of $\bar{\rm u} \neq \bar{\rm d}$ is not yet entirely clear. The *Pauli exclusion principle* would suggest that the creation of $\rm u\bar{u}$ pairs is indeed suppressed relative to $\rm d\bar{d}$ pairs because of the excess of u over d valence quarks. However, it is difficult to translate this observation into a prediction for the *shape* of $\bar{\rm d}/\bar{\rm u}$. A more likely explanation is that there is a non-negligible contribution to the cross-section from scattering off a *meson cloud* surrounding the nucleon target. In particular, if the amplitude for ${\rm p} \to \pi^- + \Delta^{++}$ is suppressed relative to that for ${\rm n} \to \pi^- + {\rm p}$, which appears to be the case, then effectively $\bar{\rm u} < \bar{\rm d}$ in the target, in agreement with the Drell–Yan data. For a detailed discussion of the phenomenology of this see, for example, the work of Melnitchouk *et al.* (1999), and references cited therein.

While models of this type appear to account satisfactorily for the observed increase of $\bar{\rm d}/\bar{\rm u}$ from 1 as x increases from 0 to about 0.15, they have difficulty in accommodating the apparent turnover of the ratio at higher x, see figure 7. One firm conclusion that can be drawn from figure 7 is that more-precise data at higher x are badly needed!

4. Precision phenomenology at hadron colliders: W and Z production

We end this review with an example of how hadron–hadron interactions can achieve a very high level of precision in testing the Standard Model. In this case, parton distributions measured very accurately in deep-inelastic scattering are *inputs* into the hard-scattering cross-section.

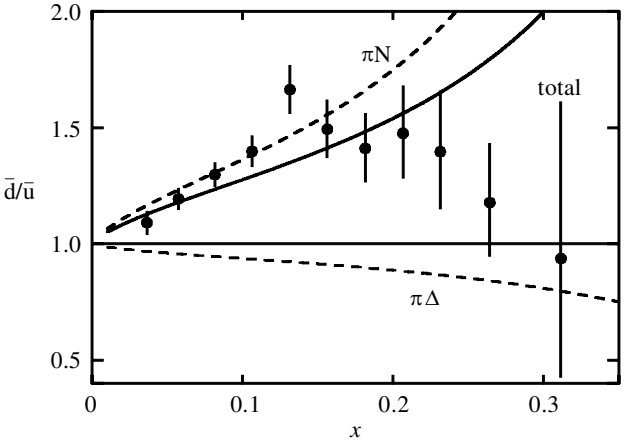

Figure 7. A comparison of the predictions of a 'meson cloud' model for the parton ratio $\bar{\mathrm{d}}/\bar{\mathrm{u}}$ with data from the E866 collaboration (from Melnitchouk *et al.* 1999). The separate contributions from the πN and πΔ states are shown (dashed lines), together with the total (solid line).

In fixed-target Drell–Yan production, the masses of the lepton pairs are typically $M_\psi \lesssim M_{\mathrm{l}^+\mathrm{l}^-} \lesssim \mathcal{O}(20\ \mathrm{GeV})$. If the hadron collision energy is large enough, for example at the high-energy $\mathrm{p\bar{p}}$ colliders, the annihilation of quarks and antiquarks can produce real W and Z bosons. Indeed, the discovery in 1983 of the W and Z gauge bosons in this way at the CERN $\mathrm{p\bar{p}}$ collider (Arnison *et al.* 1983; Banner *et al.* 1983) provided dramatic confirmation of the Glashow–Salam–Weinberg electroweak model.

The decay widths of the W and Z are $\mathcal{O}(2\ \mathrm{GeV})$, and so, instead of the differential distribution in the resulting lepton pair (lν or $\mathrm{l}^+\mathrm{l}^-$) invariant mass, it is more appropriate to consider the cross-sections for the production of approximately stable on-shell particles with masses M_W and M_Z. These can then be multiplied by branching ratios for the various hadronic and leptonic final states. In analogy with the Drell–Yan cross-section derived above, the subprocess cross-sections for W and Z production are readily calculated to be

$$\left.\begin{aligned}\hat{\sigma}^{\mathrm{q\bar{q}}'\to\mathrm{W}} &= \tfrac{1}{3}\pi\sqrt{2}G_\mathrm{F}M_\mathrm{W}^2|V_{\mathrm{qq}'}|^2\delta(\hat{s}-M_\mathrm{W}^2),\\ \hat{\sigma}^{\mathrm{q\bar{q}}\to\mathrm{Z}} &= \tfrac{1}{3}\pi\sqrt{2}G_\mathrm{F}M_\mathrm{Z}^2(v_\mathrm{q}^2+a_\mathrm{q}^2)\delta(\hat{s}-M_\mathrm{Z}^2),\end{aligned}\right\} \tag{4.1}$$

where $V_{\mathrm{qq}'}$ is the appropriate Cabibbo–Kobayashi–Maskawa matrix element, and v_q (a_q) is the vector (axial vector) coupling of the Z to the quarks.

The theoretical technology for calculating the total W and Z cross-sections is relatively robust. The $O(\alpha_\mathrm{s})$ perturbative QCD correction to the W and Z cross-sections is the same as the Drell–Yan correction (for a photon of the same mass) discussed in the previous section: the gluon is 'flavour blind' and couples in the same way to the annihilating quark and antiquark. Indeed, as already noted, these cross-sections are now known to next-to-next-to-leading-order (NNLO), i.e. $O(\alpha_\mathrm{s}^2)$ (Hamberg *et al.* 1991*a*, *b*; van Neerven & Zijlstra 1992). For Z production, the complete set of $\mathcal{O}(\alpha)$ electroweak corrections are also known (Baur *et al.* 1998)—the analysis mirrors that of Z production at LEP1—whereas for W production the QED (i.e. photon emission) part of the full $\mathcal{O}(\alpha)$ correction has been calculated (Baur *et al.* 1999). The residual theoretical uncertainty from unknown electroweak corrections is estimated to be below $\mathcal{O}(1\%)$.

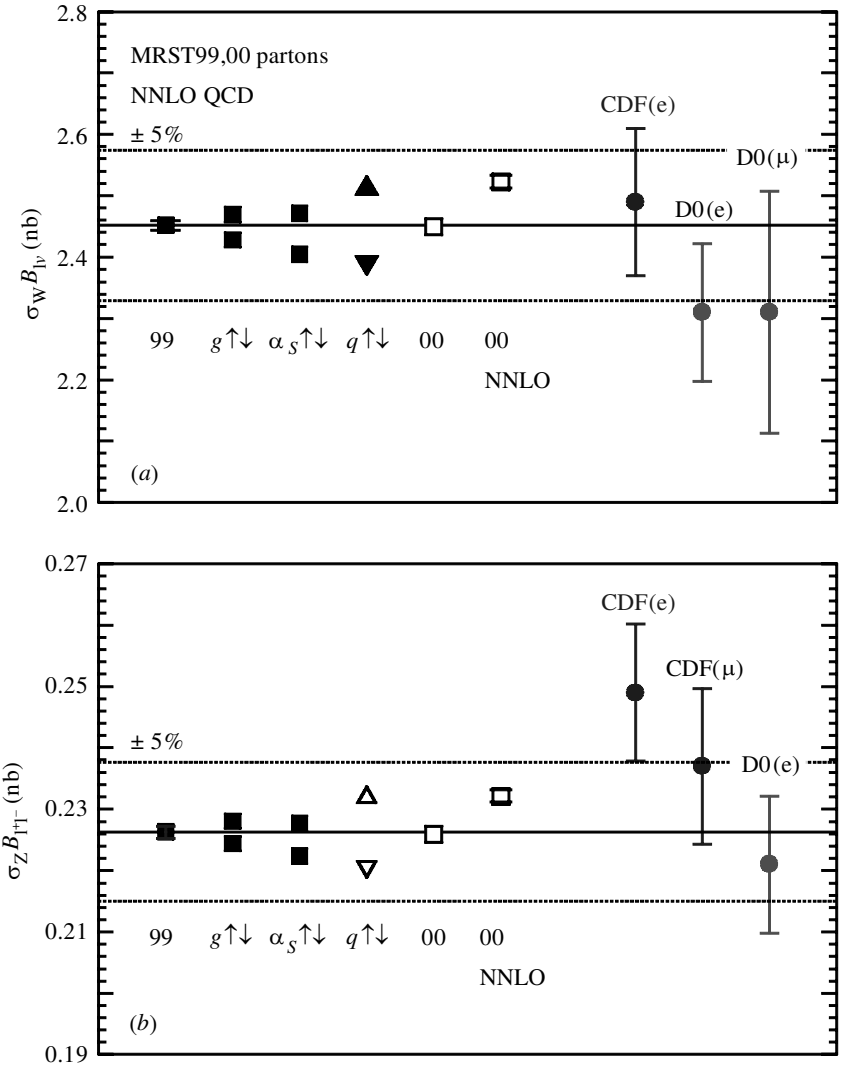

Figure 8. Theoretical predictions based on MRST partons (Martin *et al.* 2000*a*) for (*a*) W and (*b*) Z cross-sections at the Tevatron, compared with data from CDF (Abe *et al.* 1999*a*, *b*; Affolder *et al.* 2000) and D0 (Abbott *et al.* 1999). Predictions labelled '00' correspond to new preliminary NLO and NNLO MRST fits (see Martin *et al.* 2000*b*).

The main theoretical uncertainty, therefore, originates in the input parton distribution functions and, to a lesser extent, from α_s.† For the hadro-production of a heavy object like a W boson, with mass M and at central rapidity, leading-order kinematics give $x \sim M/\sqrt{s}$ and $Q^2 \sim M^2$. Notice that u,d quarks with x values typical of Tevatron and LHC production are already more or less directly 'measured' in deep-inelastic scattering (in fixed-target experiments and at HERA, respectively), but at much lower Q^2. Therefore, the two important sources of uncertainty in the parton distribution functions relevant to W, Z production are:

† The two are of course correlated.

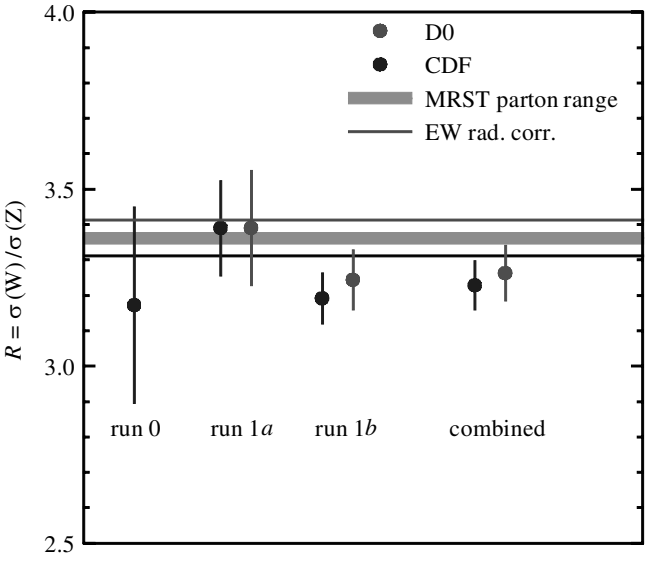

Figure 9. The ratio of W and Z total cross-sections (i.e. without branching ratios) at the Tevatron. The data are obtained assuming $B(\mathrm{W} \rightarrow \mathrm{e}\nu)/B(\mathrm{Z} \rightarrow \mathrm{ee}) = 3.2155 \pm 0.0060$, and the theoretical prediction is from Martin *et al.* (2000*a*).

(i) the uncertainty in the DGLAP evolution, which, except at high x, comes mainly from the gluon and α_s, and

(ii) the uncertainty in the quark distributions from measurement errors on the structure function data used in the fit.

In order to investigate these effects, variants of the standard MRST99 distributions have been constructed (Martin *et al.* 2000*a*), allowing the effect of approximate $\pm 1\sigma$ variations in the gluon, α_s, the overall quark normalization, and the s and c parton distributions on the W and Z cross-sections to be quantified. A comparison of the resulting predictions with the latest CDF (Abe *et al.* 1999*a*, *b*; Affolder *et al.* 2000) and D0 (Abbott *et al.* 1999) measurements at the Tevatron $\mathrm{p\bar{p}}$ collider is shown in figure 8. Evidently, the largest variation in the predictions (*ca.* $\pm 3\%$) comes from the effect of the normalization uncertainty in the input structure function data. Overall, $\pm 5\%$ would appear to be a conservative estimate of the theoretical uncertainty.† Note that an important component of the experimental error is due to the luminosity measurement and uncertainty. The latter is quoted as $\pm 3.6\%$ for CDF and $\pm 5.4\%$ for D0. In addition, the value assumed for the total $\mathrm{p\bar{p}}$ cross-section is slightly different (by 6.2%) for the two experiments, and this may account in part for the systematically smaller D0 cross-sections displayed in figure 8. Predictions for the LHC pp collider have similar theoretical errors (Martin *et al.* 2000*a*), which raises the interesting possibility of using W and Z cross-sections as 'luminosity monitors' at this machine.

It is interesting to consider the *ratios* of the W and Z cross-sections in figure 8. These are experimentally much more precisely measured, since the luminosity cancels

† Note that the most recent 'standard' MRST and CTEQ distributions, MRST99(1)—the central prediction in figure 8 —and CTEQ5M1 (Lai *et al.* 2000), give almost identical cross-sections.

in the ratio. Many of the theoretical uncertainties, for example the overall structure function normalization error, also cancel. The predictions in figure 8 use Standard Model values for the partial and total decay widths to calculate the branching ratios. For the Z, these widths are very precisely pinned down by LEP1 data. However, the total W decay width is still rather poorly determined experimentally, and so the W/Z cross-section ratio provides an interesting indirect measurement:

$$R = \frac{N(\mathrm{W} \to \mathrm{e}\nu)}{N(\mathrm{Z} \to \mathrm{ee})} = \frac{B(\mathrm{W} \to \mathrm{e}\nu)}{B(\mathrm{Z} \to \mathrm{ee})}\frac{\sigma(\mathrm{W})}{\sigma(\mathrm{Z})} = \frac{\Gamma(\mathrm{W} \to \mathrm{e}\nu)\Gamma_{\mathrm{Z}}}{\Gamma(\mathrm{Z} \to \mathrm{ee})\Gamma_{\mathrm{W}}}\frac{\sigma(\mathrm{W})}{\sigma(\mathrm{Z})}. \tag{4.2}$$

Figure 9 shows data on the cross-section ratio $\sigma(\mathrm{W})/\sigma(\mathrm{Z})$ from CDF and D0, obtained by dividing the ratio of observed leptonic events by the Standard Model prediction $B(\mathrm{W} \to \mathrm{e}\nu)/B(\mathrm{Z} \to \mathrm{ee}) = 3.2155 \pm 0.0060$. The band on the theoretical prediction is an estimate of the uncertainty due to parton distributions (coming mainly from the d/u ratio), and the lines correspond to an estimated $\pm 1\%$ uncertainty from electroweak radiative corrections. The comparison between theory and experiment is intriguing, as there is some slight hint of a disagreement. When this is translated into a measurement of Γ_{W}, one finds (Lancaster 1999)

$$\Gamma_{\mathrm{W}}(\mathrm{CDF} + \mathrm{D0}, \mathrm{indirect}) = 2.171 \pm 0.027(\mathrm{stat.}) \pm 0.056(\mathrm{sys.})\ \mathrm{GeV}, \tag{4.3}$$

to be compared with the Standard Model prediction of $\Gamma_{\mathrm{W}} = 2.0927 \pm 0.0025$ GeV.

I am grateful to my collaborators Alan Martin, Richard Roberts and Robert Thorne for providing much of the material used in this paper.

References

Abbott, B. *et al.* 1999 Measurement of W and Z boson production cross sections. *Phys. Rev.* D **60**, 052003.

Abe, F. *et al.* 1999*a* Measurement of Z^0 and Drell–Yan cross sections using dimuons in $\bar{p}p$ collisions at $\sqrt{s} = 1.8$ TeV. *Phys. Rev.* D **59**, 052002.

Abe, F. *et al.* 1999*b* Measurement of $\sigma B(\mathrm{Z}^0 \to \mathrm{e}^+\mathrm{e}^-)$ in $\mathrm{p\bar{p}}$ collisions at $\sqrt{s} = 1.8$ TeV. *Phys. Rev. Lett.* **76**, 3070.

Affolder, T. *et al.* 2000 The transverse momentum and total cross section of $\mathrm{e}^+\mathrm{e}^-$ pairs in the Z-boson region from $\mathrm{p\bar{p}}$ collisions at $\sqrt{s} = 1.8$ TeV. *Phys. Rev. Lett.* **84**, 845.

Arneodo, M. *et al.* 1994 A re-evaluation of the Gottfried sum. *Phys. Rev.* D **50**, 1.

Arnison, G. *et al.* 1983 Experimental observation of isolated large transverse momentum energy electrons with associated missing energy at $\sqrt{s} = 630$ GeV. *Phys. Lett.* B **122**, 103.

Aurenche, P. *et al.* 1989 The gluon content of the pion from high p_{T} direct photon production. *Phys. Lett.* B **233**, 517.

Baldit, A. *et al.* 1994 Study of the isospin breaking in the light quark sea of the nucleon from the Drell–Yan process. *Phys. Lett.* B **332**, 244.

Banner, G. *et al.* 1983 Observation of single isolated electrons of high transverse momentum in events with missing transverse energy at the CERN $\bar{p}p$ collider. *Phys. Lett.* B **122**, 476.

Baur, U., Keller, S. & Sakumoto, W. K. 1998 QED radiative corrections to Z boson production and the forward backward asymmetry at hadron colliders. *Phys. Rev.* D **57**, 199.

Baur, U., Keller, S. & Wackeroth, D. 1999 Electroweak radiative corrections to W boson production in hadronic collisions. *Phys. Rev.* D **59**, 013002.

Best, C. *et al.* 1997 Pion and rho structure functions from lattice QCD. *Phys. Rev.* D **56**, 2743.

Drell, S. D. & Yan, T. M. 1970 Massive lepton-pair production in hadron–hadron collisions at high energies. *Phys. Rev. Lett.* **25**, 316.

Ellis, S. D. & Stirling, W. J. 1991 Constraints on isospin breaking in the light quark sea from the Drell–Yan process. *Phys. Lett.* B **256**, 258.

Ellis, R. K., Stirling, W. J. & Webber, B. R. 1996 *QCD and collider physics.* Cambridge University Press.

Glück, M., Reya, E. & Vogt, A. 1992 Pionic parton distributions. *Z. Phys.* C **53**, 651.

Hamberg, R., Matsuura, T. & van Neerven, W. L. 1991*a* The contribution of the gluon–gluon subprocess to the Drell–Yan K-factor. *Nucl. Phys.* B **345**, 331.

Hamberg, R., Matsuura, T. & van Neerven, W. L. 1991*b* A complete calculation of the $O(\alpha_{\mathrm{S}}^2)$ correction to the Drell–Yan K-factor. *Nucl. Phys.* B **359**, 343.

Hawker, E. A. *et al.* 1998 Measurement of the light antiquark flavor asymmetry in the nucleon sea. *Phys. Rev. Lett.* **80**, 3715.

Lai, H. L. *et al.* 2000 Global QCD analysis of parton structure of the nucleon: CTEQ5 parton distributions. *Eur. Phys. J.* C **12**, 375.

Lancaster, M. 1999 Electroweak measurements from hadron machines. In *19th Int. Symp. on Lepton and Photon Interactions at High-Energies (LP 99), Stanford, CA, August 1999.* Preprint hep-ex/9912031.

Martin, A. D. *et al.* 1992 Parton distributions for the pion extracted from Drell–Yan and prompt photon experiments. *Phys. Rev.* D **45**, 2349.

Martin, A. D. *et al.* 1998 Parton distributions: a new global analysis. *Eur. Phys. J.* C **4**, 463.

Martin, A. D. *et al.* 2000*a* Parton distributions and the LHC: W and Z production. *Eur. Phys. J.* C **14**, 133.

Martin, A. D. *et al.* 2000*b* Estimating the effect of NNLO contributions on global parton analyses. Preprint hep-ph/0007099.

Melnitchouk, W., Speth, J. & Thomas, A. W. 1999 Dynamics of light antiquarks in the proton. *Phys. Rev.* D **59**, 014033.

Moreno, G. *et al.* 1991 Dimuon production in proton–copper collisions at $\sqrt{s} = 38.8$ GeV. *Phys. Rev.* D **43**, 2815.

Owens, J. F. 1984 Q^2 dependent parametrizations of pion parton distribution functions. *Phys. Rev.* D **30**, 943.

van Neerven, W. L. & Zijlstra, E. B. 1992 The $\mathcal{O}(\alpha_{\mathrm{s}}^2)$ corrected Drell–Yan K-factor in the DIS and MS scheme. *Nucl. Phys.* B **382**, 11.